CHALMERS

The Effect of Gadolinium on the Dissolution of Uranium Dioxide in Synthetic Ground Water under Simulated Early-Stage Repository Conditions

Master of Science Thesis in Nuclear Chemistry

ZHIBO MA

Department of Chemical and Biological Engineering
Division of Nuclear Chemistry
CHALMERS UNIVERSITY OF TECHNOLOGY
Gothenburg, Sweden, 2013
Report No. KKR131017

The Effect of Gadolinium on the Dissolution of Uranium Dioxide in Synthetic Ground Water under Simulated Early-Stage Repository Conditions

Master of Science Thesis

Zhibo Ma

Department of Chemistry and Biotechnology

Division of Nuclear Chemistry

CHALMERS UNIVERSITY OF TECHNOLOGY

Göteborg, Sweden, 2013

The Effect of Gadolinium on the Dissolution of Uranium Dioxide in Synthetic Ground Water under Simulated Early-Stage Repository Conditions

ZHIBO MA

Nuclear Chemistry
Department of Chemistry and Biotechnology
CHALMERS UNIVERSITY OF TECHNOLOGY
Göteborg, Sweden 2013

The Effect of Gadolinium on the Dissolution of Uranium Dioxide in Synthetic Ground water under Simulated Early-Stage Repository Conditions

ZHIBO MA

Technical Report No. KKR131017
Nuclear Chemistry
Department of Chemistry and Biotechnology
Chalmers University of Technology
SE-412 96 Göteborg
Sweden
Telephone + 46736815869

Göteborg, Sweden 2013

Contents

1 Abstract

In the Swedish model of nuclear waste repository, spent nuclear fuel pellets are finally encapsulated in iron-copper canisters and then deposited in crystalline basement rocks. Water might intrude into this repository system and get contaminated due to the dissolution of uranium. To prevent the dissolution of uranium in underground water is important. The mechanism of uranium dissolution is yet to be fully understood. It is found that under some conditions, for example, when H_2, who is produced in the repository system, and ε-particles, who are among the most important fission products, both exist, uranium dissolution is significantly suppressed.

It is possible that under other conditions, uranium dissolution might also be reduced. This project investigates the effect of Gd, who represents the lanthanides, on the dissolution of uranium in synthetic underground water under early-stage repository conditions.

The results of the experiments show that the dissolution of uranium is significantly reduced or at least postponed when Gd is present. However, the dissolution of uranium in this project is much higher than other similar experiments. Further experiments with more accurate conditions can be performed.

Key words: spent nuclear fuel repository, uranium dissolution, effect of gadolinium

2 Theory

2.1 Nuclear power and nuclear fuel wastes

Nuclear power makes use of the energy released by nuclei fission. Today in the field of civil electricity generation, the main fission material is ^{235}U.

Natural uranium consists of more than 99.2% ^{238}U and only 0.72% ^{235}U. In order to be used in a reactor, nature uranium must be enriched up to reactor-grade, to contain 3-4% 235U. The reason for enrichment is that only ^{235}U in natural uranium is fissile, while ^{238}U who dominates the composition of natural uranium is not. The eventual product of uranium enrichment is UO_2, which is made into fuel pellets. After use in the nuclear reactor, the spent nuclear fuel still contains more than 95% UO_2, though various fission products are produced through the reactions. [1]

The masses of most fission products in nuclear fuel range from 60 to 160, with two peaks occuring around 95 and 140. Many of the fission products, as well as ^{235}U and ^{238}U, are radioactive.

When nuclear fuels are spent out, they must be properly deposited due to their radioacitivity.

2.2 Repository environment of nuclear fuel wastes

2.2.1 The three barriers of the final repository

According to the Swedish laws, spent nuclear pellets are classified as high-level radioactive wastes due to their high radioactivity, and must be isolated from human and natural environment before their radioactivity drops to a low enough level. Newly spent nuclear fuels are highly radioactive and warm, so must be placed in water storage pools which act as a radiation shield and coolant. After about one year, they are transferred to SKB´s (Svensk Kärnbränslehantering AB) interim storage facility (also called Clab) in two storage pool systems 30 metres down in the bedrock.

Radioactivity and heat generation in the fuels are reduced over time, but the spent fuels would not be deemed safe until very long time (up to 100,000 years or even more) later. Interim storage facility isn't capable to offer long time isolation, therefore the spent nuclear fuels would be eventually deposited in the final repository. [2,3]

The final repository is required to function for at least 100,000 years, and for 1 million years if better. During this period, the spent nuclear fuels are expected to be isolated from human and natural environment. After such a long period, the radioactivity of the wastes significantly drops. [3]

The key point for a long-term repository is to make sure that the fuel does not dissolve. Because once the fuel gets dissolved, radioactive particles may be spread into the environment via the underground water. Therefore the spent fuel should be isolated from underground water. To achieve this goal, a method for the final repository (100,000 years isolation) is developed. The spent nuclear fuels will be protected by three barriers – from the innermost to the outermost – the canister, the buffer and the rock.

The furthest left part of Figure 1 shows the look of a spent nuclear fuel rod. Queued pellets are wrapped with fuel cladding. After interim storage, fuel rods are encapsulated into specially designed impermeable canisters, as shown in the second left part of Figure 1. Such a canister is nearly five metres long and over a metre in diameter, and weighs between 25 and 27 tonnes when

filled with spent nuclear fuel. The canister is made of two casings. The outer casing is a five-centimetre-thick layer of copper to protect against corrosion. Inside is a nodular cast iron insert that provides additional strength. [3,4,5]

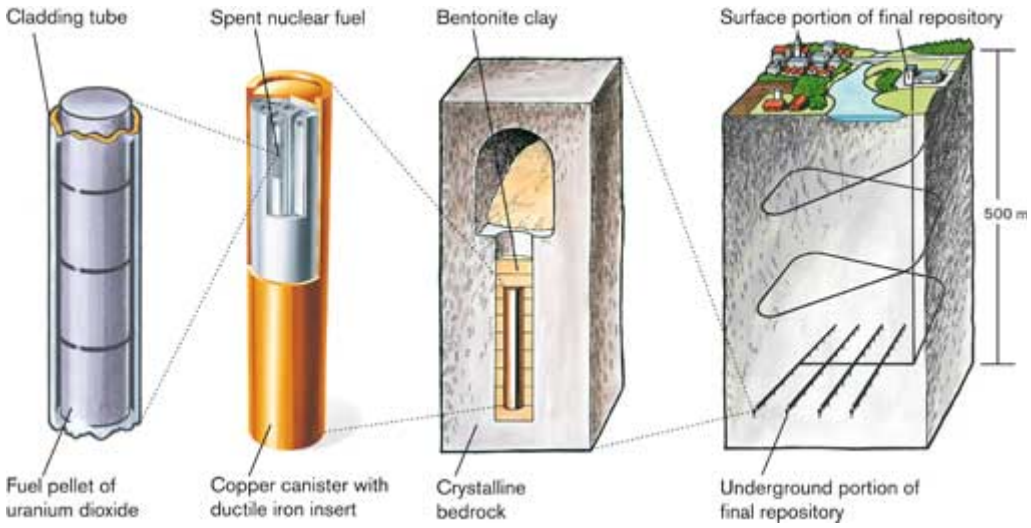

Figure 1 [5] – Repository of spent nuclear fuel, from left to right (microscopy to macroscopy)

The canisters that encapsulate the spent nuclear fuel rods are to be lowered into the final repository's deposition holes. The rest of the holes will be filled with bentonite clay, as shown in the third left part of Figure 1. The bentonite clay will act as a buffer between the walls of the deposition hole and the copper canister, which damps both mechanical movements and chemical changes in the rock. Also, once a canister becomes permeable, the buffer is expected to delay the spread of radioactive substances that may escape. The deposition holes are about 500m underground. [3,5,6]

The rock surrounding the final repository, as shown in the furthest right part of Figure 1, will serve to isolate the waste from man and the environment, and to offer the canister and the bentonite clay buffer a stable chemical environment and protect them from whatever is happening at ground level. [4]

The chosen site for spent fuel repository should be in an environment that has been stable for billions of years. In such an environment, it is possible to make predictions on development in the very long term. The Swedish crystalline basement rock meets the requirement. The final repository site would be close to the Forsmark nuclear power plant, while SKB's interim storage facility for spent nuclear fuel is in Oskarshamn. In Äspö Hard Rock Laborary, different technical solutions in a real environment are tested on a full-scale. [7,8]

2.2.2 Water intrusion might happen

Even if well-protected by the threefold barriers, the spent nuclear fuels are not 100% isolated, because fractures may be caused by various reasons, for example, manufacture failure of the canister, corrosion to the canister, or geological changes of the rocks that lead to the geometrical changes of the canisters. In fact no design is forever safe. Once a fracture is formed,

water has chance to intrude into the canister and interact with the pellets and get contaminated.

It would cause trouble if contaminated underground water flows out of the fractured canister and return to the biosphere, as the radioactive components dissolved in the water would be carried out and spread to the near environment causing further contamination. To avoid this, it is required to restrain the contamination of underground water. It is hence necessary to investigate how the contamination happens inside the canister.

2.3 The interactions between water and the spent nuclear fuels

It is mentioned in section 2.1, after use in the nuclear reactor, the spent nuclear fuel still contains more than 95% UO_2, and mentioned in section 2.2.1, the key point for a long-term repository is to make sure that the fuel does not dissolve. Moreover, 95% of the radiotoxic fission products are trapped in the UO_2 matrix, and can be released when UO_2 gets dissolved. [9] The release of fission products is not wanted either. Therefore the core issue of many recent researches is to investigate the dissolution of UO_2 in underground water under final repository conditions.

2.3.1 Reducing conditions inside the canisters

Several years after the repository system is closed, reducing conditions will prevail in the environment inside the canister, because the oxidants (mainly free O_2) that get in during the construction are consumed by reducing minerals and bacteria. Once underground water intrudes into the canister, under anoxic conditions, it will corrode the iron, the inner layer material of the canister, to produce reductant H_2 through the reactions below: [10,11]

$$Fe + 2H_2O \leftrightarrow Fe^{2+} + 2OH^- + H_2\,(g) \qquad \textit{Equation 1}$$

$$3Fe + 4H_2O \leftrightarrow Fe_3O_4 + 4H_2\,(g) \qquad \textit{Equation 2}$$

Although the reactions above are supposed to be equilibrium, the backward reactions would not occur before H_2 pressure reaches the order of 100 Mpa. The H_2 pressure therefore can be expected to reach a very high level. [10]

2.3.2 Local oxidizing conditions close to the fuel

Although generally reducing conditions will prevail in the repository condition, close to the spent fuel surface (in a distance of some micrometer), the local redox condition can be oxidizing, because the inherent radioactivity of the spent nuclear fuel will induce radiolysis of the underground water in contact with the fuel, producing equal amounts of oxidants and reductants. [12,13] For kinetic reasons, the oxidants will have the larger effect on the local environment. [14] Major oxidizing species are H_2O_2, $OH\cdot$, $HO_2\cdot$ and O_2, among them the most important oxidant is H_2O_2. [15]

2.3.3 Oxidation and dissolution of U

Dissolution of UO_2 and spent nuclear fuel under repository conditions has been extensively studied. However, as the system is very complex, it can be difficult to draw any mechanistic conclusions from experiments using spent nuclear fuel. To circumvent this problem, one way is to study the elementary processes involved using simple model systems. [1]

In UO_2, uranium exists in the form of U(IV), who has low solubility in water. However, U(IV) can be oxidized by oxidants to U(VI), who is more than 1000 times more soluble. [16] It is U(VI) who is much more threatening to contaminate the underground water. Under the repository conditions, the oxidation of U(IV) to U(VI) might happen.

The studies by M. Jonsson et al. investigates the effects of various radiolytic oxidants. UO_2 pellets of same composition are immersed into carbonate solutions. Then solutions are purged and saturated with Ar, N_2O, N_2O/O_2 (80/20 mol%), air or O_2, then irradiated. It is found that for γ-irradiated systems saturated with Ar, air or O_2, the most important oxidant is H_2O_2, while for N_2O and N_2O/O_2 saturated systems the most important oxidant is $CO_3^{\bullet-}$. For α-irradiated systems, the most important oxidant is H_2O_2. Especially, the dissolution rate of uranium is significantly higher for the O_2- and air-saturated solutions where production of $O_2^{\bullet-}$ is enhanced. [17]

It is also found that the dissolution of uranium is enhanced with the presence of HCO_3^- which forms strong and water soluble complexes with UO_2^{2+}. [18] When HCO_3^-/CO_3^{2-} is not sufficient, precipitants would be formed on the surface of uranium pellets. [19]

2.3.4 The effects of H_2

H_2 inside the canisters is produced in two ways. The first, as indicated in Equation 1 and Equation 2 in section 2.3.1, is the anoxic corrosion of iron by water. The second, as mentioned in section 2.3.2, is due to the radiolysis of water, which produces both oxidants and reductants, and H_2 is one of the reductants. The former way produces more H_2 than the latter. [1]

Many studies suggest that the existence of H_2 significantly inhibit the dissolution of uranium in spent nuclear fuels in water. The mechanism of the inhibition is yet to be fully understood.

The study by T. Eriksen et al. investigates the effect of H_2 on oxidative dissolution of fragments of irradiated PWR fuel. The fragments are immersed in 0.01 mol×dm^{-3} $NaHCO_3$ (pH 8.2) solution equilibrated with either Ar, 7% H_2/93% Ar or 30% H_2/70% Ar at a pressure of 0.1 Mpa. H_2 was found to reduce the rate of O_2 formation, while the concentration of H_2O_2 remains the same through all the experiments. The concentration of U in the solution after 20 days leaching was lower in the presence of H_2 than in purely Ar saturated solution, the effect being more pronounced when H_2 takes more pressure share. [20]

2.3.5 The effects of ε-particles

Fissions in nuclear fuels produce various products. The atomic mass of fission products are most likely around 95 or 140. [21,22] Fission products like Mo, Ru, Tc, Rh, Pd and Te gather in spent fuels and form clusters which are often referred to as ε-particles. Some of the suggested elements, such as Ru, Rh and Pd are noble metals.

Some recent studies suggest that the presence of noble metal ε-particles may affect the influence of H_2 on uranium dissolution.

The study by D.W. Shoesmith et al. compares the behaviours of SIMFUEL specimens with and without incorporated noble metal ε-particles under H_2, Ar or O_2 atmosphere. The result shows that with the presence of both H_2 and ε-particles, the corrosion potential of SIMFUEL is significantly reduced and the corrosion response is slowed; with the presence of both O_2 and ε-particles, the corrosion potential, on the contrast, is increased; while without the presence of ε-particles, H_2 alone doesn't make substantial change in corrosion potential. This means ε-particles may act as catalytic electrodes for H_2 oxidation, $H_2 \leftrightarrow 2e^- + 2H^+$, as well as the oxidation of uranium by O_2. [23]

The study by M. Trummer et al. investigated the effects of Pd on the kinetics of radiation induced dissolution of spent nuclear fuel. The experiments were performed using UO_2 pellets containing 0%, 0.1%, 1% and 3% Pd as a model for spent nuclear fuel. The pellets were immersed in aqueous solution containing H_2O_2 who was used as a model for radiolytical oxidants (previous studies have shown that H_2O_2 is the most important oxidant in such systems) and HCO_3^-, then sealed under H_2 atmosphere of different pressures. The consumption of H_2O_2 and the dissolution of uranium were analyzed as a function of H_2 pressure (0–40 bar). Pd is found to catalyse the oxidation of UO_2 as well as the reduction of surface bound oxidized UO_2 by H_2. In both cases the rate of the process increases with increasing Pd content. [1]

2.4 The study in this project

As mentioned in section 2.3.5, the atomic mass of fission products in nuclear fuels are most likely around 95 and 140, and Pd is proved to have co-effect on the dissolution of uranium in underground water. Since many of the products whose atomic masses are around 140 are lanthanides, it seems reasonable to expect some effect of lanthanides on the dissolution of uranium. It can be interesting to investigate the effects of lanthanides on the dissolution of uranium in spent nuclear fuel. In this project, we use Gd as a representative of lanthanides to perform a preliminary investigation.

Two kinds of pellets, containing Gd or not, are used in this project. The pellets are immersed into synthetic underground water after surface treatment, and then sealed in simulated waste fuel repository environment. The synthetic water is sampled on certain days and the concentration of uranium in the synthetic water on each sampling day is examined by ICP-MS (ICP-MS does not measure the concentration directly, but detects the intensity of plasmas which is proportional to the concentration of uranium).

By comparing the uranium concentrations of the two kinds of pellets on each day, the effect of Gd can be seen and some preliminary conclusions can be drawn.

3 Experimental

3.1 Parameters of the pellets

Ten uranium pellets of two kinds are prepared for the project. The two kinds are “pure pellets” (4 pellets in total) which contain pure UO_2 and “Gd pellets” (6 pellets in total) which contain UO_2 and 2% Gd. The 10 pellets are numbered into two groups, as “pure pellets” pA – pD, and “Gd pellets” GdA – GdF. The basic parameters of each kind of pellets are listed in Table 1.

According to the data in Table 1, the surface/volume (S/V) ratio can be calculated. For pure pellets, the S/V ratio is roughly $0.585 m^{-1}$; for Gd pellets, the S/V ration is roughly $0.685 m^{-1}$.

Table 1 – Basic parameters of the two kinds of pellets to be investigated*

kind	pure pellet	Gd pellet
number	4	6
diameter (mm)	~9.95	~8.2
length (mm)	~10.92	~10.13
weight (g)	8.22	5.32
proportion of UO_2 (%)	100	98
proportion of Gd (%)	0	2
enrichment of ^{235}U (%)	1.96	0.72

* Pellets pB and GdE are chosen as representatives of respective kinds of pellets to measure the diameters and lengths. In fact they are the only two whose diameter and length are measured. While the weight of all the pellets are measured, and in the table shows the average weight of each kind of pellet. The proportion of UO_2, proportion of Gd and the enrichment of ^{235}U are given by the company that provides the pellets.

3.2 Instruments and experimental procedures — SEM

3.2.1 The first microscopy

The 10 pellets are microscoped to check the surface composition. Microscopy is performed by Quantax 70, an SEM (Scanning Electron Microscope) instrument. The SEM is a microscope that uses electrons instead of light to form an image. Quantax 70 is equipped for software Hitachi TM3000 to present the formed imaged on computer screen.

Each pellet is microscoped three times, each time from a different surface — the top side, the under side or the lateral side.

Some representative results of first microscopy are shown in Table 2 and Figure 2. The under surface of pellet pA (Figure [a]) and top surface of pellet GdB (Figure [b]) are taken as representatives. For each single pellet, the compositions of all three surfaces are similar; for the pellets of the same kind, the compositions of their surfaces are similar.

As shown in Table 2 and Figure 2, it is seen that in untreated pellets, regardless of containing Gd or not, the ratios between U(uranium) atom counts and O(oxygen) atom counts in pure pellets' surfaces and gadolinium pellets' surfaces are roughly the same, both around (U:O=1:2), the ratio in gadolinium pellets' is slightly lower. In both pellets' surface layers, C (carbon) is found by the machine. But this is probably an instrumental error, since neither of the two kinds of pellets contains any carbon. Another possible instrumental error is that the U:O ratio in pellet pA's surface, which is higher than 1:2. This is not so likely, as the major component of the pellets is UO_2, and U(IV) tends to be oxidized in the air, lowering the U:O ratio.

The composition of surfaces of other pellets show similar results.

Table 2 – Composition of raw pellets' surfaces shown by microscopy.

[a] The under surface of pure pellet pA. [b]The top surface of Gd pellet GdB.

[a]		[b]	
Element	Atom count percent (%)	Element	Atom count percent (%)
U	29.49	U	25.28
O	48.29	O	52.66
Gd	–	Gd	1.98
C	22.23	C	20.09

[a] [b]

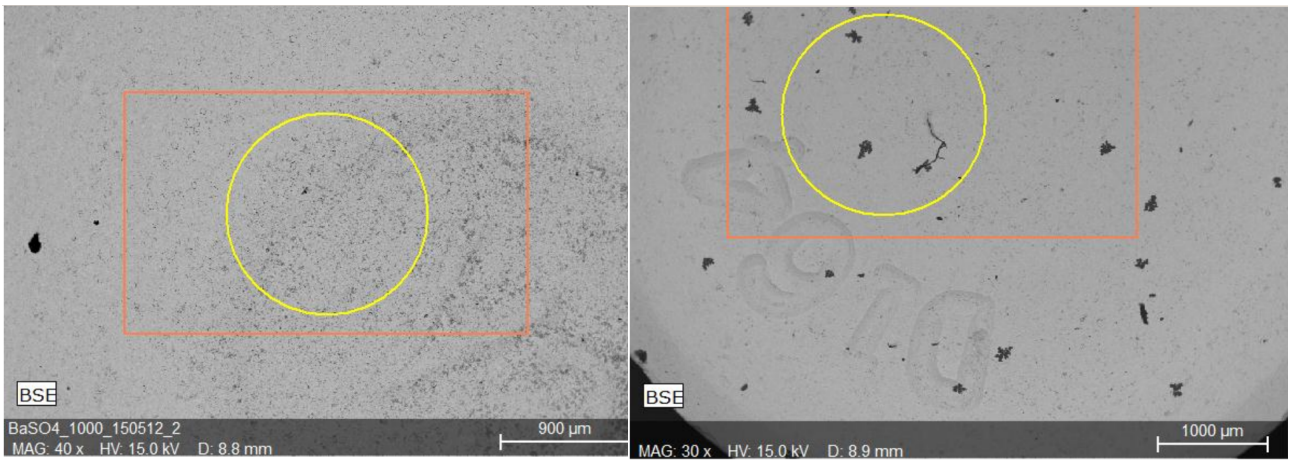

Figure 2 – SEM image of raw pellets' surfaces shown by microscopy.

[a] The under surface of pure pellet pA. [b] The top surface of Gd pellet GdB.

3.2.2 Surface treatment to the pellets

After laid aside for some time, the ten pellets are immersed into 200ml 1mM $NaHCO_3$ solution in a plastic bottle. The $NaHCO_3$ solution is then manually purged with abundant N_2, to drive out the dissolved O_2 In the solution. Then the bottle is immediately sealed and gently vibrated to increase contact. $NaHCO_3$ forms strong aqueous U-carbonate complexes with U(VI), which is highly mobile and soluble. [24] In this way, the oxidized surface layer is supposed to be removed from the pellets. The immersion lasts 72 hours, after which period pellets pA and GdB are microscoped again, with the other pellets staying in the $NaHCO_3$ solution. After the surface treatment, the likely oxidized surface layers of the pellets are supposed to be removed.

3.2.3 The second microscopy

The results of second microscopy are shown in Table 3 and Figure 3.

Table 3 presents similar composition to Table 2, and the images in Figure 3 and Figure 2 resemble in pair. The (U:O) ratio of treated GdB is slightly higher than the ratio of raw GdB. This is

perhaps because of the fact that after removal of old oxidized surface layer whose (U:O) is usually lower than 1:2, the new oxidized layer is not fully formed yet; or purely instrumental uncertainty. The (U:O) ratios of treated pA and raw pA are very closed to each other, the former slightly higher. This is most likely due to instrumental uncertainty.

GdB and pA are put back into the $NaHCO_3$ solution after their second microscopy and are immersed for another 27 hours to remove the re-oxidized surface layer. The bottle is again sealed and vibrated gently.

The other eight pellets are never taken out of the solution during this part of the experiment.

Table 3 – Composition of $NaHCO_3$-treated pellets' surfaces shown by microscopy.

[a] The under face of pure pellet pA. [b]The top face of Gd pellet GdB.

[a]		[b]	
Element	Atom count percent	Element	Atom count percent
U	29.20	U	25.04
O	49.39	O	51.34
Gd	–	Gd	2.24
C	21.41	C	21.38

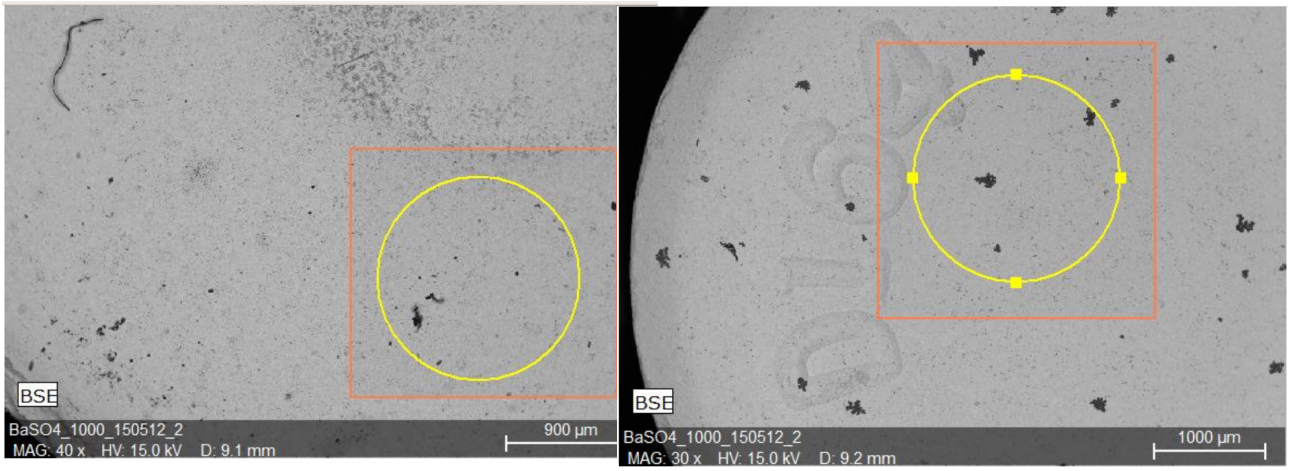

Figure 3 – Photos of $NaHCO_3$-treated pellets' surfaces shown by microscopy.

[a] The under face of pure pellet pA. [b] The top face of Gd pellet GdB.

3.3 Instruments and experimental procedures — Leaching

3.3.1 Pressure vessel

After being immersed in the $NaHCO_3$ solution for another 27 hours, all the ten pellets are individually placed into simulated repository conditions. Gd pellets first, followed by pure pellets.

Each pellet is to be encapsulated into a pressure vessel, which readily contains 30ml synthetic water. Both kinds of pellets can be fully immersed by the synthetic water. The inner space of the pressure vessel is not fully filled. The unfilled space is left for high-pressured hydrogen.

The structure of a sealed pressure vessel is shown in Figure 4 [a] and [b] in section 3.3.3.

The inner surface of pressure vessel is made of PEEK, namely polyether etherketone, to minimize adsorption of U.

3.3.2 Synthetic water

The synthetic water is used to simulate the local underground water (500m underground) near Äspö Hard Rock Laboratory. The composition of the synthetic water is listed in Table 4.

Table 4 * [25,26] – The composition of the synthetic water that simulates the underground water at Äspö

chemical	molmass	g/L	mol/L
NaCl	58.4	4.59	7.86E-02
Na_2SO_4	142	0.751	5.29E-03
$SrCl_2•6H_2O$	267	0.0242	9.06E-05
KCL	74.6	0.0635	8.51E-04
NaBr	103	0.0283	2.75E-04
$NaHCO_3$	84	0.171	2.04E-03
Na_4SiO_4	184	0.0341	1.85E-04
$MgCl_2$ **	95	0.908	9.56E-03
$CaCl_2•4H_2O$ **	181	4.223	2.33E-02

*Only the components whose concentrations are higher than 1mg/L are used.

**The originally suggested chemicals in the reference are $MgCl_2•H_2O$ and $CaCl_2•2H_2O$, which are not found in the chemical storage and therefore replaced by $MgCl_2$ and $CaCl_2•4H_2O$ respectively. The composition of the synthetic water is not affected in this way because any "$•xH_2O$" melts in water solution.

3.3.3 High-pressured H_2 inside pressure vessels

As mentioned, in the repository, reducing conditions generally prevail, and H_2 is produced. The air pressure of H_2 inside the canisters would be high. The existence of high-pressured H_2 in the pressure vessels simulates the real environment in the repository and helps to keep the reducing conditions.

The structure of pressure vessel is shown in Figure 4 [a]. Synthetic water (B area in Fig 5 [a]) doesn't fill the whole inner space of the vessel, but occupies roughly 2/3 of the whole inner space when immersing the pellet. The rest of the inner space, namely the upper part (A area in Fig 5 [a]), is air when the vessel is just sealed. And some air is inevitably dissolved in the synthetic water

because the water contacts air.

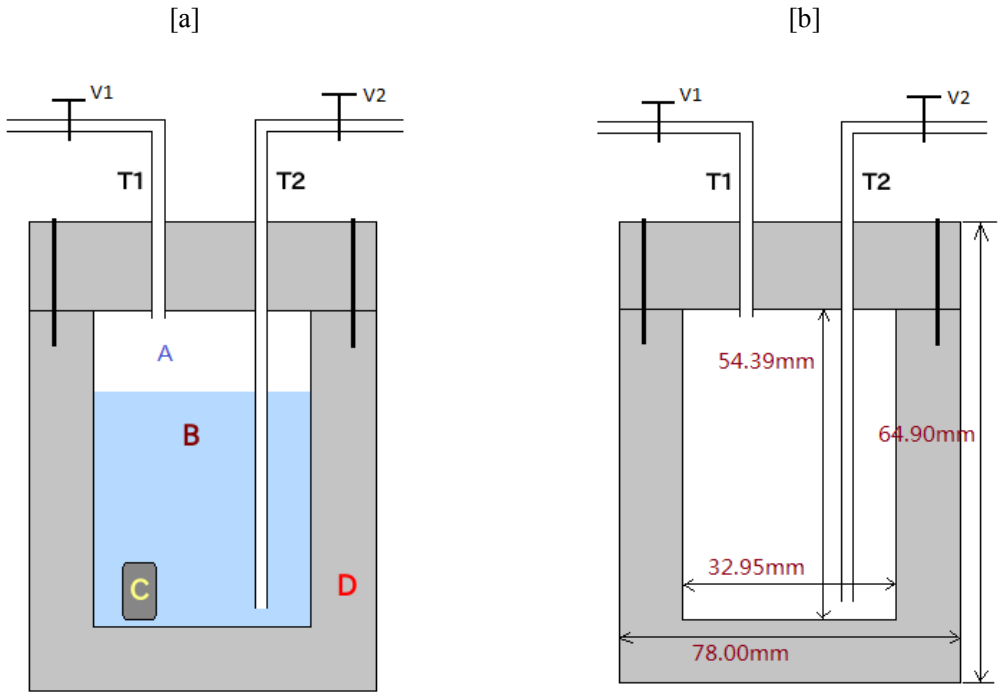

Figure 4 – The structure of pressure vessel used in the experiment

[a] The structure of a sealed pressure vessel with fuel pellet and synthetic water in it. *T1 and T2 are tubes that connect the inside and outside of the vessel, and V1 and V2 are respectively their valves. A, B and C respectively stand for the gas space, the synthetic water and the pellet. The grey area, D, is the vessel.

[b] The parameters of the structure of a pressure vessel.

Immediately after the pellet and synthetic water is sealed in the pressure vessel, V1 and V2 are opened and hydrogen is pumped into the vesesel through T2 for a while. In this way, small part of the hydrogen is dissolved in the synthetic water, while the majority of the hydrogen goes through synthetic water and the gas space, then leaves the vessel through T1. In this way, the air that is left in the vessel and dissolved in the synthetic water is partly driven away by the strong flux of hydrogen. After a while, V1 is closed while hydrogen is still pumped in until the gas pressure in the vessel reaches maximum, 3 bars. Then V2 is also closed therefore the vessel is utterly sealed. All the ten pressure vessels are pressurized in this same way. The reducing conditions inside the copper canisters in the repository is therefore simulated.

3.3.4 Numbering the pressure vessels

Each pressure vessel is numbered according to the respective pellet contained. The pressure vessels containing "Gd pellets" are numbered as GdA – GdF, and the "pure pellets" are numbered as pA – pD. The pellets take the number of the pressure vessels respectively.

3.3.5 Sampling

Since the moment the pellet is dropped into the synthetic water, uranium dissolution starts. The synthetic water that contains dissolved uranium is namely the leaching solution. Each leaching solution is numbered, taking the same number of the pressure vessel that contains it. For example, pressure vessel pA contains leaching solution pA and pellet pA, and pressure vessel GdB contains leaching solution GdB and pellet GdB.

To investigate the dissolution of uranium under the simulated repository environment, one must sample and check the composition of the leaching solution. To do this without losing the reducing conditions inside the pressure vessels, one must sample the leaching solution without opening the pressure vessels.

When sampling is performed, V2 is opened and the leaching solution is pumped out through T2 by the high-pressured hydrogen inside the vessel. The small vials are marked with the date of sampling and which vessel the sample comes from. Each time after sampling, V2 is immediately closed. If it is necessary to replenish the gas pressure, V1 is opened and extra hydrogen is pumped in through T1 until the pressure reaches 3 bars.

The sampled leaching solution is called “original sample”. Each original sample is numbered according to its respective leaching solution and the date when it is fetched. For example, the original sample fetched from leaching solution pC on the 6th day is numbered as “pC-6”, and the original sample fetched from leaching solution GdD on the 15th day is numbered as “GdD-15”.

The 10 over-pressurized vessels simulating repository conditions are kept for 70 days from the day when they are firstly sealed on. On the 1st, 3rd, 6th, 10th, 15th, 22nd, 29th, 41st, 45th, 51st, 57th, 63rd and 69th day after sealing, sampling is performed. On the 1st, 3rd and 6th day, the vessels are re-pressurized after sampling. GdA is out of work since the 1st day and pA is out of work since the 57th day due to pressure loss.

3.4 Instruments and experimental procedures — ICP-MS measurement

ICP-MS (Inductively Coupled Plasma Mass Spectrometry) measures the plasma intensity of decided isotopes in solution which is proportional to the concentration of the isotopes. In this project, the isotopes to be checked are ^{235}U, ^{236}U, ^{238}U and ^{232}Th. As the dilution of uranium is a chemical property which is independent on the neutron number, it is the concentration of uranium the element, namely the sum of the concentrations of ^{235}U, ^{236}U and ^{238}U that is mainly cared.

3.4.1 Dilution

Raw samples from the vessels cannot be measured by ICP-MS directly due to the potential high concentration. Solutions with high radioactivity might contaminate the instrument, and if the concentration is too high, the detector might get saturated and have “dead time” problems thus miss some signals. Therefore, they samples must be diluted for measurement. Internal standards and external standards are used to help do the measurement.

1M HNO_3 that contains 10ppb ^{232}Th as the internal standard is used for all the dilution.

Each sample is expected to be diluted to 100, 1000 and 10000 times, therefore the concentration of diluted samples are roughly 1/100, 1/1000 and 1/10000 of the original sample respectively.

10ppM U solution is expected to be diluted to 100ppb, 50ppb, 10ppb, 1ppb and 0.1ppb. These diluted U solutions are to be used as external standards. The acid consumption for the dilution is large, so 4 bottles of 1M HNO_3 are used. The 4 acids are numbered AA, BB, CC and dd respectively.

Due to the accuracy limit of volume-measuring tools (pipettes for example), the dilution cannot be precise as wanted (such as 1/100 and 10ppb), but is somewhere around that. With the help of electronic scale, the real dilution can be calculated. For instance, the mass of a sample is calculated by the mass of the vial containing this sample minus the mass of this vial when it is empty, while the mass of the acid used to dilute this sample is calculated by the mass of the vial containing both the sample and acid minus the mass of the vial containing only the sample. The mass densities of the acid with and without sample in it are closely the same, as the volume of the sample is far smaller than the acid to dilute it. Therefore the ratio between masses of the acid with and without the sample is regarded as the ratio between their volumes. The same applies to the dilution of 1ppM U solution.

The real dilution D is given by Equation 5 as below.

$$D=\frac{V_s}{V_s+V_{ac}}=\frac{m_s/\rho}{m_s/\rho+m_{ac}/\rho}=\frac{m_s}{m_s+m_{ac}} \qquad \textit{Equation 5}$$

$$m_s=m_{s+v}-m_v$$

$$m_{ac}=m_{ac+s+v}-m_{s+v}$$

In the equations above, each term stands for:

V_s: The volume of original sample/10ppM U solution

V_{ac}: The volume of 1M HNO_3 acid

ρ: The mass density. The mass density of 1M HNO_3 and any sample, original or diluted, are considered the same.

m_s: The mass of original sample/10ppM U solution

m_{ac}: The mass of 1M HNO_3

m_v: The mass of an empty vial

m_{s+v}: The mass of a vial containing only original sample/10ppM U solution

m_{ac+s+v}: The mass of a vial containing original sample/10ppM U sollution, and also 1M HNO_3 for dilution

Each external standard solution is numbered according to the acid used to dilute it and its expected concentration. The real concentration differs slightly from the expected concentration. For example, external standard solution “AA-50ppb” is diluted by acid AA and is expected to be diluted to 50ppb. Due to the accuracy limit of the pippet, it is not diluted to exactly 50ppb. Its real concentration after dilution is 50.94ppb, which is gained by calculation.

The exact concentration of each external standard solution is shown below in Table 5.

Table 5 – List of the U concentration of each external standard

Number	Real concentration (ppb)	Number	Real concentration (ppb)
AA-100ppb	101.1	CC-100ppb	102.5
AA-50ppb	50.94	CC-50ppb	51.29
AA-10ppb	9.801	CC-10ppb	10.32
AA-1ppb	1.361	CC-1ppb	1.445
AA-0.1ppb	0.099	CC-0.1ppb	0.105
BB-100ppb	102.4	DD-100ppb	101.8
BB-50ppb	51.50	DD-50ppb	51.05
BB-10ppb	10.14	DD-10ppb	6.852
BB-1ppb	1.377	DD-1ppb	1.365
BB-0.1ppb	0.102	DD-0.1ppb	0.070

Each diluted sample is numbered according to the number of original sample, the date when it is fetched and the expected dilution. The 1M HNO_3 that is used to dilute it is also declared. For example, the diluted sample of original sample GdD on the 45th day which is expected to be diluted 100 times is numbered as “GdD-45-100-AA”, and the diluted sample of original sample pB on the 22nd which is expected to be diluted 1000 times is numbered as “pB-22-1000-CC”. They are diluted by acid AA and acid CC respectively, and the expected dilutions are not exactly the real.

The real dilution of the diluted samples will be listed in Table 7 in section 3.4.2. It is not mentioned here because some more details would be clarified.

3.4.2 How ICP-MS works

The solution to be measured flows inside the concentric channels of the ICP torch, and gets ionized by the high voltage when a spark is applied inside the torch. The ions from the plasma are then extracted through a series of cones into a mass spectrometer, usually a quadrupole. The ions are separated on the basis of their mass-to-charge ratio and a detector receives an ion signal proportional to the concentration.

3.4.2 Measurement

The concentration of uranium in any leaching solution is expected to increase all the way during the 70 days. Therefore it is expected that for any leaching solution, its original sample on the 1st day has the lowest concentration among all its original samples, and the sample on the 69th day has the highest. Therefore, by measuring the concentrations of the samples on the 1st day and the concentrations of the samples on the 69th day, one can roughly ascertain the concentration ranges of the samples.

The diluted samples (1/100, 1/1000 and 1/10000) of pD and GdF on the 1st, 10th and 69th day are measured in advance, to estimate the approximate range of the concentration ranges of the samples.

It is found that the U concentrations of all the three 1000-time-diluted samples of pD and the three 100-time-diluted samples of GdF fall into the measuring range (0.1ppb to 10ppb) and are not close to either border. As the U concentrations of the same kind of samples on the same day are expected not to differ too much from each other, this means it is enough to measure only the 1000-time-diluted samples of pure original samples and 100-time-diluted samples of Gd original samples. Moreover, the intensity of 50ppb external standard and 100 ppb standard exceeds the maximum scale range of ICP-MS, therefore they are not used. Table 6 shows the detailed measurement of ICP-MS on each sample.

Table 6 * – Detailed measurement of ICP-MS on each sample.

sample	date												
	1	3	6	10	15	22	29	41	45	51	57	63	69
pA													
pB	1000	1000	1000	1000	1000	1000	1000	1000	1000	1000	1000	1000	1000
pC	1000	1000	1000	1000	1000	1000	1000	1000	1000	1000	1000	1000	1000
pD		1000	1000		1000	1000	1000	1000	1000	1000	1000	1000	
GdA													
GdB	100	100	100	100	100	100	100	100	100	100	100	100	100
GdC	100	100	100	100	100	100	100	100	100	100	100	100	100
GdD	100	100	100	100	100	100	100	100	100	100	100	100	100
GdE	100	100	100	100	100	100	100	100	100	100	100	100	100
GdF		100	100		100	100	100	100	100	100	100	100	

*100 Samples only whose 100-time-diluted solutions are measured by ICP-MS. 1000 Samples only whose 1000-time-diluted solutions are measured. Samples all of whose diluted solutions are measured. Samples who are not measured due to pressure fail. The vessels of these two samples soon lost pressure after sealing.

Each diluted samples is numbered according to the original sample, the expected dillution time, and the date when the sample is fetched. The acid used to dilute it is also declared.

The real concentration of each measured diluted sample is listed below in Table 7.

Table 7 – The real concentrations of each measured dilluted sample

Number of the diluted sample	Real dilution	Number of the diluted sample	Real dilution
GdB-100-1-dd	106.45	GdF-100-1-dd	101.87
GdB-100-3-dd	106.34	GdF-100-3-dd	99.55
GdB-100-6-CC	98.50	GdF-100-6-CC	100.31
GdB-100-10-dd	112.85	GdF-100-10-dd	101.87
GdB-100-15-CC	100.48	GdF-100-15-CC	100.82

GdB-100-22-CC	104.66	GdF-100-22-CC	104.75
GdB-100-29-AA	99.13	GdF-100-29-AA	97.20
GdB-100-41-AA	99.15	GdF-100-41-AA	98.29
GdB-100-45-AA	99.02	GdF-100-45-AA	97.69
GdB-100-51	98.92	GdF-100-51	99.03
GdB-100-57	99.43	GdF-100-57	98.73
GdB-100-63	99.21	GdF-100-63	101.11
GdB-100-69	98.28	GdF-100-69-dd	102.62
GdC-100-1-dd	107.64	pB-1000-1-dd	1008.63
GdC-100-3-dd	105.72	pB-1000-3-dd	1064.37
GdC-100-6-CC	98.48	pB-1000-6-CC	1128.96
GdC-100-10-dd	100.09	pB-1000-10-dd	990.05
GdC-100-15-CC	103.51	pB-1000-15-CC	974.68
GdC-100-22-CC	107.61	pB-1000-22-CC	1001.35
GdC-100-29-AA	99.47	pB-1000-29-AA	972.66
GdC-100-41-AA	98.46	pB-1000-41-AA	955.10
GdC-100-45-AA	98.78	pB-1000-45-AA	947.48
GdC-100-51-BB	98.24	pB-1000-51-BB	973.91
GdC-100-57-BB	98.85	pB-1000-57-BB	975.95
GdC-100-63-BB	105.21	pB-1000-63-BB	1090.13
GdC-100-69-dd	96.66	pB-1000-69-CC	924.67
GdD-100-1-dd	105.89	pC-1000-1-dd	1213.00
GdD-100-3-dd	104.41	pC-1000-3-dd	1052.29
GdD-100-6-CC	99.03	pC-1000-6-CC	996.45
GdD-100-10-dd	99.74	pC-1000-10-dd	1073.24
GdD-100-15-CC	100.58	pC-1000-15-CC	977.43
GdD-100-22-CC	105.92	pC-1000-22-CC	1058.21
GdD-100-29-AA	99.36	pC-1000-29-AA	973.04
GdD-100-41-AA	99.58	pC-1000-41-AA	968.69
GdD-100-45-AA	98.81	pC-1000-45-AA	962.66
GdD-100-51-BB	97.91	pC-1000-51-BB	981.29
GdD-100-57-BB	98.69	pC-1000-57-BB	969.31
GdD-100-63-BB	107.22	pC-1000-63-BB	1097.95
GdD-100-69-dd	100.83	pC-1000-69-CC	981.03
GdE-100-1-dd	104.26	pD-1000-1-dd	1129.88

GdE-100-3-dd	100.68	pD-1000-3-dd	1087.30
GdE-100-6-CC	99.32	pD-1000-6-CC	964.67
GdE-100-10-dd	111.81	pD-1000-10-dd	989.62
GdE-100-15-CC	101.76	pD-1000-15-CC	960.48
GdE-100-22-CC	105.69	pD-1000-22-CC	1035.12
GdE-100-29-AA	99.29	pD-1000-29-AA	983.54
GdE-100-41-AA	98.11	pD-1000-41-AA	965.99
GdE-100-45-AA	99.46	pD-1000-45-AA	962.99
GdE-100-51-BB	99.37	pD-1000-51-BB	978.17
GdE-100-57-BB	98.84	pD-1000-57-BB	982.79
GdE-100-63-BB	115.84	pD-1000-63-BB	1013.02
GdE-100-69-dd	97.85	pD-1000-69-CC	960.66

Samples/Standards in the same group are measured together. For each measurement batch, the blank, namely the acid used to dilute this batch, is measured first, followed by the external standards from the lowest concentration to the highest. Samples are measured in the last, from the "Gd samples" to the "pure samples", and from the ones on the earliest date to the last date. An example of the measuring sequence of a batch is listed below in Table 8. This batch uses acid AA as for dilution, therefore naked acid AA is measured first as the blank.

3.4.5 Calculation

ICP-MS measures the plasma intensity of certain isotopes, which is proportional to the concentration of these isotopes in the solution. When the solution does not contain any uranium, the intensity given by ICP-MS would be zero. In this way, if the concentration-intensity relation of the solution is adjusted in a Cartesian coordinate system, a linear line crossing the origin can be drawn.

For each batch, the real concentration of U in each external standard is calculated; the intensity of U in each external standard is measured by ICP-MS.

In the preliminary measurement, it is found that the intensities of 50ppb and 100ppb U solution is beyond the maximum measurement range of the ICP-MS, and no valid result is given. Therefore the 50ppb and 100ppb external standards are withdrawn. Some of the 0.1ppb external standards show abnormally high intensity of U, these results are also removed.

Table 8 – An example of the measuring subsequence of a batch

Subsequence of measurement	Number of the measured blank / standard / sample	Subsequence of measurement	Number of the measured blank / standard / sample
1	Blank acid AA	12	GdE-45-100-AA
2	AA-0.1ppb	13	GdF-45-100-AA

3	AA-1ppb	14	pB-29-1000-AA
4	AA-10ppb	15	pC-29-1000-AA
5	GdD-29-100-AA	16	pD-29-1000-AA
6	GdE-29-100-AA	17	pB-41-1000-AA
7	GdF-29-100-AA	18	pC-41-1000-AA
8	GdD-41-100-AA	19	pD-41-1000-AA
9	GdE-41-100-AA	20	pB-45-1000-AA
10	GdF-41-100-AA	21	pC-45-1000-AA
11	GdD-45-100-AA	22	pD-45-1000-AA

The concentrations and intensities of the 1ppb and 10ppb external standards are used to calculate the concentration of U in the diluted samples. Chart 1 below is taken as an example to show how the calculation is performed. A Cartesian coordinate is set, x-axis giving intensity values and y-axis giving concentration values. The concentrations and intensities of the 1ppb and 10ppb external standards are adjusted in this coordinate system. The origin (0,0) is also adjusted, reflecting the solution contains no uranium if the intensity gives zero. A linear trend line is regulated by these three points. This trend line theoretically crosses the origin.

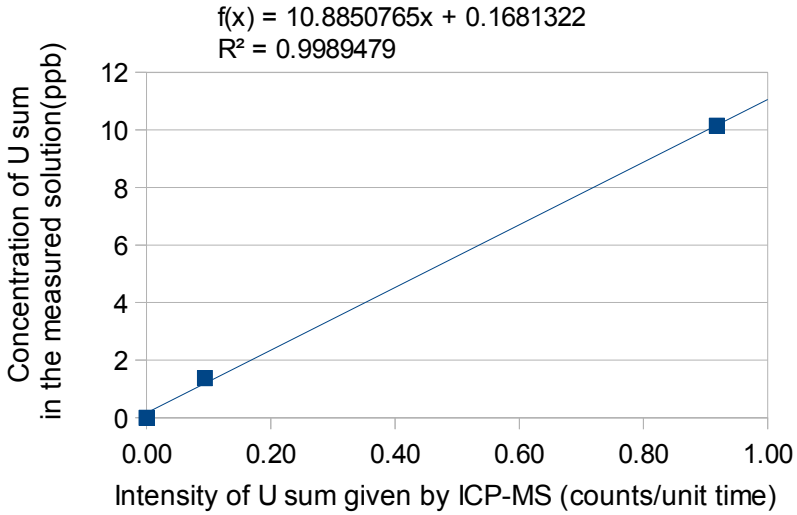

x values in the chart above	y values in the chart above
0.00000	0.00000
0.09384	1.37686
0.91821	10.14374

Chart 1 – An example of deciding the linear relation between intensity of U sum given by ICP-MS and the concentration of U sum in the measured solution

Knowing the intensity of U in each diluted sample (given by ICP-MS), by adjusting the

intensity value to the trend line, the concentration of this diluted sample can be calculated.

The concentration of original sample can be calculated by the concentration of U in the diluted samples timing its respective dilution multiple.

Results of the ICP-MS measurement is shown in the next chapter.

4 Results and Conclusion

4.1 Results

U concentrations of pure samples, Gd samples and all measured samples are shown in Chart 2, Chart 4 and Chart 6 respectively. The concentration of each sample on each day is listed. In all the three charts, the value is the concentration of original sample. The unit of concentration is changed to “µmol/l” from “ppb”, which was used during the measurement. In Chart 2 and Chart 3, the deviation of ICP-MS measurement of each point is indicated. The average concentrations of each kind of sample on each sampling day are shown in Chart 3 and Chart 5.

In Chart 2, the concentration of sample pD on the 22nd day is lost for unknown reason. In Chart 3, the concentrations for samples GdB and GdC on the 1st, 3rd and 6th day are lost, because the background of these samples, namely the HNO_3 used to dilute them, showed abnormally high concentration of uranium, higher than any sample and external standard, making it impossible to do the calculation. These data are therefore not shown in Chart 6 either.

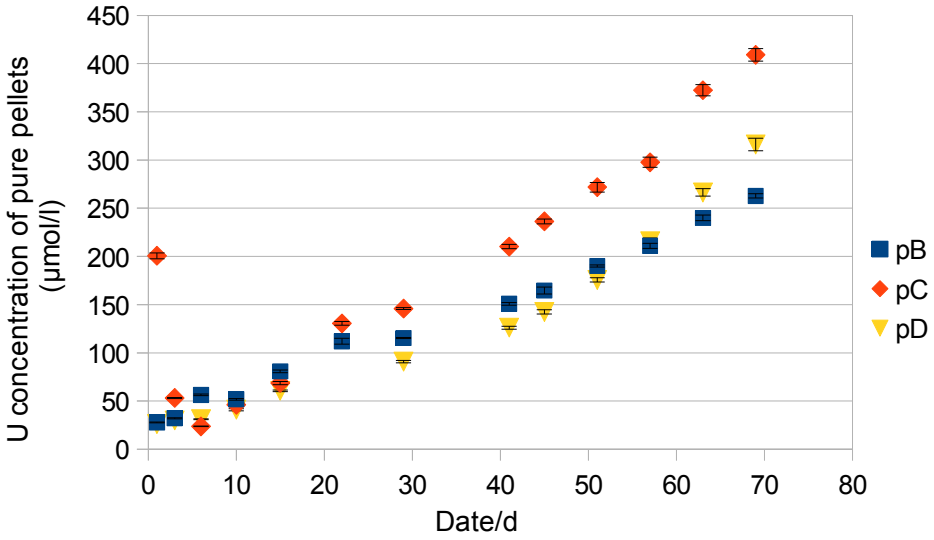

Chart 2 – U concentration of samples pB, pC and pD on each sampling day during the simulated repository period (0-70th day)

In Chart 2, it is seen that:

1) The concentration of U sum (the total concentration of ^{235}U, ^{236}U and ^{238}U) in any of the three batches (pB, pC and pD) increases steadily along with time passes, and doesn't show a trend to flat.

2) During the 22nd to the 41st day, the concentration increases slightly slower than other time intervals.

3) The initial concentrations of sample pE on the 1st and 2nd day are abnormally high. This is probably because some uranium might be stuck in the tubes of pressure vessels (see T1 and T2 in Figure 2), since the pressure vessels are previously used for other projects.

4) The curves (if the points in the same data series are smoothly connected) of the three samples almost overlap with each other during the first 29 days (If the first two points of pE are

not accounted.). Since the 41st day, the concentration of pC is higher than the other two, while the curve pB and pD go on well overlapping until the 69th day.

5) The uncertainty of each measure point is low. This is because only the uncertainty from ICP-MS measurement is given here. The uncertainty of from the concentration of external standard is not given.

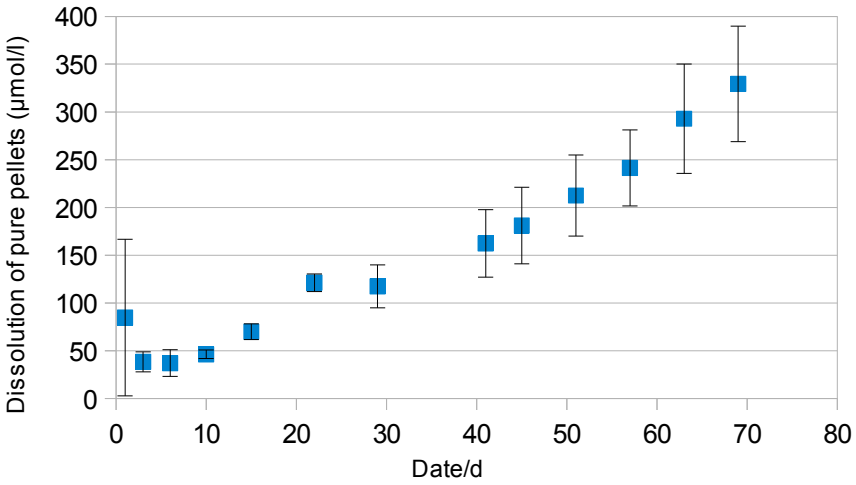

Chart 3 – The average U concentration of pure samples pB, pC and pD on each sampling day during the simulated repository period (0-70th day)

In Chart 3, it is seen that:

1) The increasing trend of U concentration is similar to the one seen in Chart 2.

2) The average concentrations on the 22nd and 29th day are very close. If more samples were taken during this period, a flat “plateau” of the curve might be seen.

3) The uncertainties of concentration on each day vary. On the 3rd, 6th, 10th and 15th day, the uncertainties (value) are low while on the other sampling days, the uncertainties (value) are higher. Since the 29th day, uncertainty (value) increases as time passes. Uncertainty (percentage) on each sampling day (except for the 1st day) mostly ranges between 7% to 19%. The uncertainty (percentage) on the 1st day, however, is very high, close to 97%. This is due to the abnormally high concentration of sample pC on the 1st day. The cause of high concentration is mentioned above.

In Chart 4, it is seen that:

1) The concentrations of each sample increase along with time passes in general. However, this increasing trend is not very obvious, and is with many reversals. The reversals are especially obvious during the 15th to 29th day for samples GdB and GdD, and during the 22nd to 41st day for sample GdC.

2) For any of the five samples, during the 15th to 41st day, the concentration increases slower than other periods.

3) The initial concentrations of sample pE on the 1st, 2nd and 6th day are abnormally high. The concentrations of samples pE and pF on the 51st day are abnormally low. These are probably

manual or instrumental fails in the measurement.

4) The curves of the samples hardly overlap each other.

5) The uncertainty of each measure point is low. Only the uncertainty from ICP-MS measurement is given here. The uncertainty of from the concentration of external standard is not given.

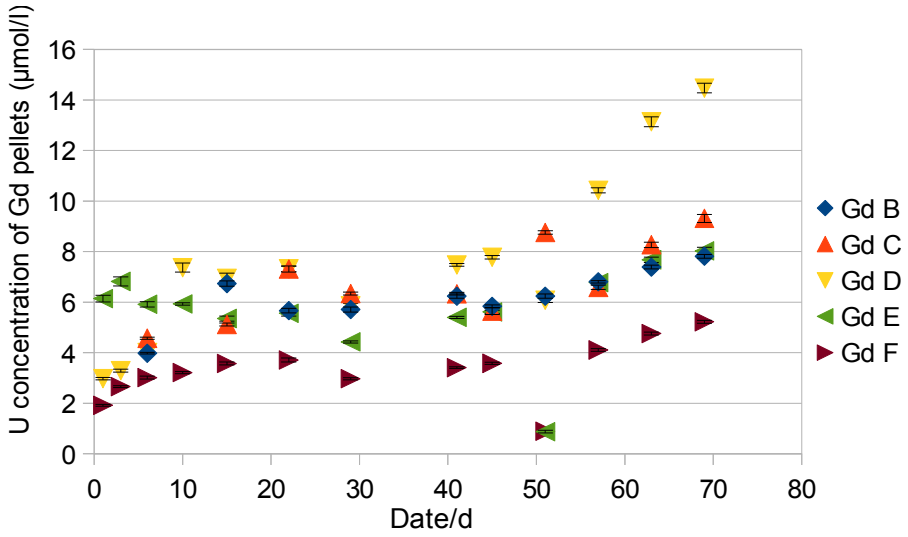

Chart 4 – U concentration of samples GdB, GdC, GdD, GdE and GdF on each sampling day during the simulated repository period (0-70th day)

In Chart 5, it is seen that:

1) The trend of U concentration increase is similar to the ones seen in Chart 4.

2) Inapparently, a flat “plateau” of the curve can be seen between the 22nd and 45th day.

3) The uncertainty (percentage) on any sampling day is higher than 22%.

It can be noticed that in Chart 2 and Chart 4, the uncertainty of the value of each point is low, while in Chart 3 and Chart 5, the uncertainty of any average value is relatively high. The high uncertainty of the average value is most likely from the uncertain conditions inside different pressure vessels.

Chart 6 shows the contrast between the concentrations of “pure samples” and “Gd samples”. In this chart, it is seen that:

1) The concentrations of the “Gd samples” are significantly lower than the concentrations of the “pure samples” since the very first day of sampling. As time passes, the difference between the concentration of the two kinds of samples increases to one or two magnitudes.

2) The concentrations of the “pure pellets” increase faster than the concentrations of “Gd pellets”. In fact, as the concentration difference between the two kinds of pellets is large, the increase of the concentration of “Gd pellets” is not easy to be noticed.

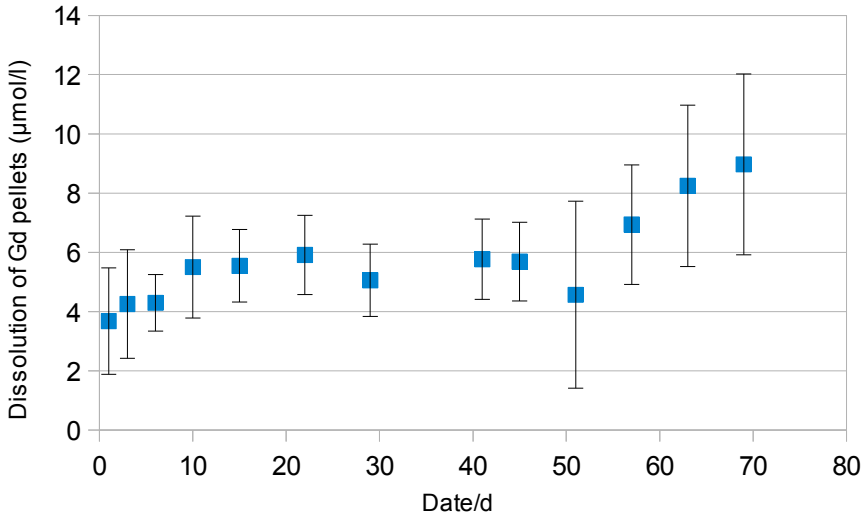

Chart 5 – The average U concentration of Gd samples GdB, GdC, GdD, GdE and GdF on each sampling day during the simulated repository period (0-70th day)

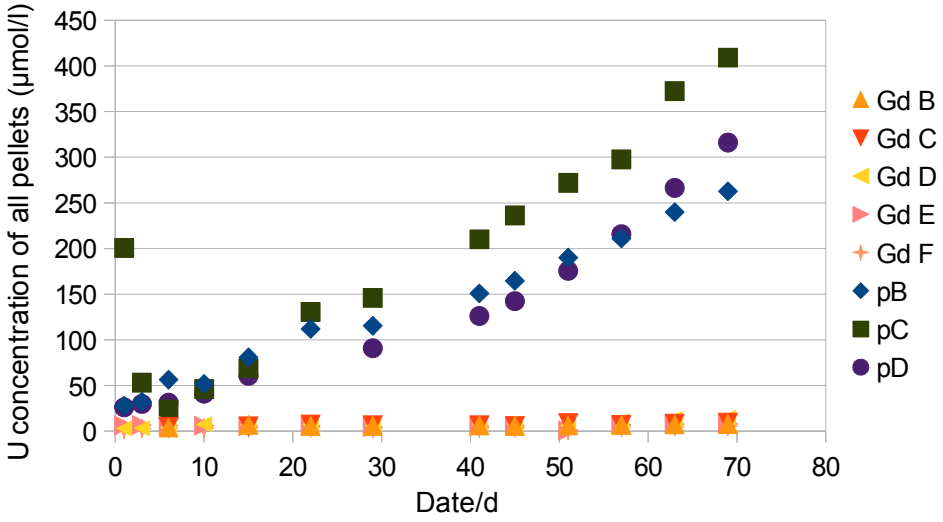

Chart 6 – U concentration of all measured samples during the simulated repository date (0-70th day)

4.2 Conclusion

The major conclusion of the project is that under simulated repository conditions, with the existence of 2% gadolinium in the pellet, less uranium is dissolved in the simulated underground water at Äspö. However, the mechanisms and rationale of this phenomena needs further investigating.

5 Discussions

5.1 The possible role played by Gd

1) Gd functions as a catalyst for the reactions between H_2 and oxidants (U(VI), radiolytical oxidants or oxidants that exists in the system), just like Pd does in other experiments. [1, 23, 27, 28] When Gd catalyzes the reaction between U(VI) and H_2, U(VI) is reduced by H_2 to U(IV) thus less uranium is dissolved. When Gd catalyzes the reactions between H_2 and oxidants other than U(VI), oxidants are consumed in the oxidation of H_2 and would not oxidize U(IV). As the solubility of U(IV) is very low, not much uranium is dissolved.

2) Gd is preferred to react with oxidants prior to U, therefore less U(IV) is oxidized to U(VI). Had this been the real situation, the rate of the reaction between Gd and oxidants must be much higher than that of the reaction between U and oxidants, because as mentioned in section 3.1 and 3.2, Gd makes up only 2% of the Gd pellets. The ratio between UO_2 and Gd is almost 50.

3) Gd may cause the formation of precipitants that contain dissolved uranium. However, no noticeable precipitant is found when some pressure vessels are opened. It is unclear if any precipitant is stuck on the pellets.

4) Gd does not play a big role, but it is the sizes of the pellets that matter. As shown in Table 1, the size of "pure pellets" is larger than that of “Gd pellets”. If the dissolution rate of uranium of unit surface area is constant, it can be expected that more uranium is dissolved during a certain period from larger pellets who has larger surfaces. This assumption is less likely because it hardly explains why the difference between the dissolutions of the two kinds of pellets is so huge, since the surface area of pure pellets is less than twice that of Gd pellets.

5) Gd does not play a big role, but it is the composition of the gas inside each pressure vessel that matters. The redox conditions inside each pressure vessel might vary. It is possible that the pure pellets are simply more exposed to dissolution-enhancing agents. This will be further discussed in section 5.2.3.

5.2 Comparison with earlier experiments in other studies

5.2.1 The existence of air inside a sealed pressure vessel

As mentioned in section 3.3.3, when a vessel is sealed, as the solution and pellets does not fill the whole space inside the vessel, there is air left in the vessel, and probably some dissolved in the solution. In order to get rid of the residual air, the vessel is purged with hydrogen immediately after sealing. However, as the method of purging the vessel is relatively primitive, it is hard to say that the residual air in the vessel can be fully cleansed. Some air is likely to survive.

Suppose the purge is very successful and all residual air is cleansed, the gas space inside the vessel should be full of 3 bar hydrogen, and the air content should be 0%. This situation is hardly achieved. Suppose the purge is very unsuccessful and no residual air is driven out, the gas space inside the vessel should be filled with 1/3 air (1 bar) and 2/3 hydrogen (2 bar), because the air pressure before purge is normal pressure, 1 bar, while the air pressure after purge is 3 bar.

Therefore, it is more reasonable to say that the air content inside the vessel after purge is somewhere between 0% – 33%, which means the oxygen content inside the vessel is somewhere between 0% – 6.6%, and the nitrogen content inside the vessel is between 0% – 26.4%. The hydrogen content is between 67% – 100%.

The existence of air inside a sealed pressure vessel might effect the redox property of the simulated repository condition thus have key effect on the dissolution of uranium. This will be discussed in section 5.2.3.

5.2.2 Comparison of dissolution

The turnouts of this project is compared to those of the works by Trummer et al.

When the pressures of H_2 (2~3 bar in this project and 1~2 bar in Trummer's experiments) and the contents of foreign substance (2% Gd in this project and 1~3% Pd in Trummer's experiments) are similar, the dissolution of uranium tends to have similar concentrations (2~8 μmol/l, mostly 4~6 μmol/l in this project and 0.6~4.3 μmol/l, mostly 3.6~4.3 μmol/l in Trummer's experiments). The difference of dissolution of the two works is less than one magnitude order.

The content of H_2 in this project is slightly higher, which means the reductant density in this project is probably higher. However, slightly more dissolution of uranium is observed in this project than Trummer's works. This is probably because:

1) This is only a matter of time. In this project, the dissolution of uranium is measured on certain days (up to the 70th day in the end) after the simulated repository condition is sealed; while in Trummers experiments, the dissolution of uranium is measured only 50 minutes after. It is possible that more uranium will be dissolved in Trummer's experiments after the 50th minute, and it is unknown how much uranium is dissolved 50 minutes after the vessel-sealing in this project.

2) The type of oxidants in the system matters. In this project, as mentioned in section 5.1 and 5.2.1, unknown amount of residual O_2 is probably present in the simulated system; while in Trummer's experiments, 2.0mM H_2O_2 are added into the system and no more oxidant is present.

5.2.3 The possible effect of air in this project

The existence of air under simulated repository conditions in this project may effect not only the experimental process, but also the outcomes of the experiments.

Due to the existence of air:

1) Reducing condition may not prevail in the sealed and pressurized vessels. This means this project is not simulating the repository condition long time (100 years or more, for example) after the closure of the real repository, when free O_2 is almost all consumed and reducing condition prevails inside the canister, but is simulating the repository condition short after the closure of the real repository.

In fact, it takes several years for the residual O_2 in the repository to be all consumed. [9] If water intrusion into the canister happens in the first several years after the canister is sealed, it is possible that H_2, O_2, N_2 and water co-exist inside a canister.

2) The existence of air accelerates the dissolution of uranium in water that contains $NaHCO_3$. This is proved in the works by E. Ekeroth et al. and M.E. Broczkowski et al. The work of the former also indicates that O_2 causes more dissolution enhancement than air, while the work of the latter indicates that ε-particles catalyse not only the reactions between H_2 and oxidants, but also the reduction of O_2 under O_2 purged conditions.

It is also noticed that in the experiments by M. Trummer et al., under N_2 purged conditions, the dissolution of uranium is enhanced when the content of N_2 is 1% and 3%. The enhancement is

more pronounced when the content of N_2 is 3%. It is not declared in the work whether N_2 acts as an oxidant to oxidize U or somehow else promotes uranium dissolution.

It can be rational to say that O_2 and N_2 both have possibility to exist and enhance the dissolution of uranium under the simulated condition in this project. The existence of the two can be an alternative explanation why the dissolution is higher in this project than in Trummer's work.

5.2.4 The uncertainties in this project

The uncertainties in this project are not small. The factors that cause uncertainties are:

1) The ICP-MS measurement. The uncertainties of ICP-MS are given in Chart 3 and Chart 5 in section 4.1. They are not big, which means the ICP-MS measurement is relatively accurate.

2) The dilution. Even if electronic scales are used to increase the accuracy of the measurement, uncertainty is always there.

3) The redox conditions inside the vessels. The amount of residual air in each pressure vessel is uncertain.

4) Others.

5.3 Extension of this project

5.3.1 Time extension

As seen in Chart 2 and Chart 4, neither batches of curves show any trend to flat in the end, though the concentration of “pure pellets” is much higher than that of “Gd pellets” and the concentration of “pure pellets” increases much faster than that of “Gd pellets”. This means 70 days may be not enough for the dissolution of uranium under the conditions in this project to reach the upper limit.

After the 70th day, if the conditions in this project is maintained, the concentration curves might:

1) gradually flat and come to a stable upper limit below saturation, owing to the presence of Gd;

2) go straight up until reaching saturation;

3) ascend even faster and reach saturation ealier.

5.3.2 Improvement of this project

Basing on this project, improved experimental conditions can be applied in order to work out finer conclusions.

1) The individual effect of H_2, O_2 and N_2 uranium dissolution can be investigated by varying the composition of gas atmosphere. It is better to have the precise content of each kind of gas.

2) The effect of Gd can be further investigated by varying the content of Gd in the pellets.

3) The effect of the components other than $NaHCO_3$ in the simulated underground water can be investigated.

4) Quantitative calculations can be made to investigate how fast the dissolution goes under various conditions.

6 Acknowledge

Thanks to professor Gunnar Skarnemark for having me as a diploma worker and leading me the way of nuclear chemistry, and especially the patience and tolerance.

To Gunnar and Louisa for always taking time to answer my questions, no matter when and what asked.

To Sravya, Stellan and Anna for all your guidance and for all the help during my many problems.

To Arvid for introducing the idea of my diploma project.

Finally I would like to direct a thank you towards all the people working at the department; you have all been very helpful and kind during these weeks and even if not all of you are mentioned by name you are all remembered.

7 References

1) Martin Trummer, Sara Nilsson, Mats Jonsson, Journal of Nuclear Materials 378 (2008) 55–59
2) SKB publication Art-205
3) SKB publication Art-141
4) SKB publication TR-11-01
5) SKB publication Art-209
6) SKB publication Art-817
7) SKB publication TR-12-03
8) SKB publication Art-119
9) Paul Carbol, Patrik Fors, Thomas Gouder, Kastriot Spahiu, Geochimica et Cosmochimica Acta 73 (2009) 4366–4375
10) Patrik Fors, 2009, Doktorsavhandlingar vid Chalmers tekniska högskola. Ny serie 2940
11) P. Carbol, P. Fors, S. Van Winckel, K. Spahiu, Journal of Nuclear Materials 392 (2009) 45–54
12) J.W.T. Spinks, R.J. Woods, An Introduction to Radiation Chemistry, John Wiley and Sons Inc., New York, 1964. 477.
13) A. Loida, V. Metz, B. Kienzler, H. Geckeis, J. Nucl. Mater. 346 (2005) 24.
14) O. Roth, M. Jonsson, Cent. Eur. J. Chem. 6 (2008) 1.
15) Ella Ekeroth, Mats Jonsson, Journal of Nuclear Materials 322 (2003) 242–248
16) Grenthe I., Fuger J., Konings R. J. M., Lemire R. J., Muller A. B., Nguyen-Trung C. and Wanner H. (1992) Aqueous uranium hydroxide complexes, crystalline and amorphous uranium oxides and hydroxides. In Chemical Thermodynamics of Uranium (eds. H. Wanner and I. Forest). North-Holland, Amsterdam., pp. 98–143.
17) Ella Ekeroth, Olivia Roth, Mats Jonsson, Journal of Nuclear Materials 355 (2006) 38 – 46
18) Mohammad Mohsin Hossain, Ella Ekeroth, Mats Jonsson, Journal of Nuclear Materials 358 (2006) 202–208
19) Bruce McNamara, Brady Hanson, Edgar Buck and Chuck Soderquist, Radiochim. Acta 93, 169 – 175 (2005)
20) T.E. Eriksen, M. Jonsson, SKB Technical Report TR-07-06, 2007, p. 1.
21) H. Kleykamp, Journal of Nuclear Materials 131 (1985) 221-246
22) http://www.world-nuclear.org/info/Nuclear-Fuel-Cycle/Introduction/Physics-of-Nuclear-Energy/#.Ug3J-RAl_cY
23) M.E. Broczkowski, J.J. Noël, D.W. Shoesmith, Journal of Nuclear Materials 346 (2005) 16–23
24) Ingemar Grenthe, J. CHEM. SOC. DALTON TRANS. 1984
25) Johan Byegård, Eva Gustavsson, Eva-Lena Tullborg, Jan-Olof Selroos, SKB R-05-86: Bedrock transport properties (Preliminary site description Forsmark area –version 1.2).
26) Johan Byegård, Eva Gustavsson, Eva-Lena Tullborg, SKB R-06-27: Bedrock transport properties - Data evaluation and retardation model (Preliminary site description Laxemar subarea – version 1.2)
27) S. Nilsson, M. Jonsson, J. Nucl. Mater. 372 (2008) 160.

28) S. Nilsson, M. Jonsson, J. Nucl. Mater. 374 (2008) 290.

8 Appendix

Table 8* – Raw results by ICP-MS measurement (intensity of isotope).

sample id	U-235	U-236	U-238	Th-232
GdB 01 100	645.2146	59.13346	14550.47	331334.4
GdB 03 100	763.2871	60.80013	19129.94	331442.1
GdB 06 100	793.1554	66.26682	23758.67	389545.7
GdB 10 100	532.0766	62.00013	17403.39	337136.3
GdB 15 100	1365.665	68.60017	38610.52	390214.2
GdB 22 100	933.6305	67.40016	31051.18	383849.4
GdB 29 100	799.8891	62.40014	26260.32	261164.7
GdB 41 100	820.6236	62.20014	29370.9	262127.1
GdB 45 100	652.9483	61.00013	27149.31	260829.9
GdB 51 100	685.4831	63.40014	29712.87	331031.9
GdB 57 100	710.8177	62.40014	32449.08	328777.8
GdB 63 100	718.5514	64.53348	36406.27	334736.2
GdB 69 100	1006.702	70.26684	56176.18	472588.2
GdC 01 100	486.675	59.26679	15263.55	334564.2
GdC 03 100	875.4935	65.06682	27356.51	336974
GdC 06 100	666.8156	68.60017	27572.38	392636.9
GdC 10 100	453.4739	64.33348	20797.66	334090.5
GdC 15 100	595.9458	65.20015	28793.52	384700.3
GdC 22 100	709.4176	68.06683	38797.02	380811.8
GdC 29 100	736.1523	61.00013	29592.49	259198.2
GdC 41 100	652.8816	59.53346	30266.5	261340.8
GdC 45 100	450.7404	61.93347	26290.58	260853.8
GdC 51 100	490.6084	61.80013	44035.03	328489.1
GdC 57 100	527.0097	61.33347	31520.34	327684.9
GdC 63 100	567.8113	62.40014	38123.74	328335.4
GdC 69 100	936.364	65.40015	71268.84	419195.4
GdD 01 100	275.2027	74.20019	15923.34	488653.6
GdD 03 100	307.4033	80.40023	18577.34	481879.7
GdD 06 100	309.0033	78.73355	19979.96	433082.7
GdD 10 100	365.2047	77.20021	25362.3	482232.9
GdD 15 100	459.2074	80.13356	40909.73	426492.6
GdD 22 100	477.008	82.80024	37984.31	428139.1
GdD 29 100	423.7396	61.53347	34119.77	325887.6
GdD 41 100	531.2099	67.60016	46410.94	332532.8
GdD 45 100	561.8111	66.20015	49151.48	333583.8
GdD 51 100	634.8141	59.66679	37445.55	428074.1
GdD 57 100	728.5519	64.20014	68784.14	431644.2
GdD 63 100	837.5579	64.86681	80727.15	431739.2

GdD 69 100	1053.372	65.80015	101526.9	428808.7
GdE 01 100	1799.313	83.33358	40841.59	487781.7
GdE 03 100	2004.274	81.0669	47883.9	484607.5
GdE 06 100	1053.772	79.53356	31242.47	427424.1
GdE 10 100	635.6808	79.53356	23243.9	478097.5
GdE 15 100	723.8184	84.73359	27220.52	424780.2
GdE 22 100	623.4136	84.20025	27214.71	427479.4
GdE 29 100	538.7435	66.13349	24098.18	329030
GdE 41 100	627.7471	62.13347	31291.1	327024.7
GdE 45 100	587.0121	65.33348	32641.65	329897.9
GdE 51 100	64.26681	62.86681	327.0038	434858.2
GdE 57 100	712.9511	66.46682	42446.98	433008.1
GdE 63 100	678.0828	65.13348	41297.42	437695.1
GdE 69 100	830.8908	62.73347	54631.96	431864.9
GdF 01 100	190.0013	78.40022	8125.644	490409.4
GdF 03 100	251.5356	72.86685	14656.05	484140.7
GdF 06 100	230.5352	80.80023	13142.44	427373.1
GdF 10 100	226.0685	75.0002	12951.07	484524.7
GdF 15 100	247.7355	76.13354	13944.67	423252.4
GdF 22 100	278.2027	79.20022	16419.17	424119.5
GdF 29 100	233.4686	65.13348	14422.41	329775.5
GdF 41 100	266.1358	59.60013	17277.24	328649.5
GdF 45 100	279.6694	67.40016	18768.59	330220.6
GdF 51 100	67.66683	60.20013	462.4742	431417.1
GdF 57 100	333.9372	63.40014	23549.13	433112.8
GdF 63 100	370.2048	65.20015	27062.28	427516.7
GdF 69 100	407.1391	64.80015	30887.96	433280.8
pA 01 1000	2501.419	112.7338	583289.9	342669.7
pA 03 1000	1848.12	95.93366	394101.3	339804.5
pA 06 1000	981.2337	66.66682	46611.87	405750.4
pA 10 1000	1343.93	78.00021	258548.8	337398.2
pA 15 1000	2338.992	102.8004	478935.9	413748.7
pA 22 1000	2274.514	104.8671	440231.3	399261.9
pA 29 1000	1843.252	95.80032	355498.4	262456.9
pA 41 1000	1670.698	88.93361	317859.6	262690.3
pA 45 1000	1606.29	87.3336	301904.4	263388.6
pA 51 1000	1773.31	89.60028	332555.4	333923.5
PB 01 1000	302.0699	74.66686	11716.6	487621.3
PB 03 1000	362.4046	79.80022	15472.71	496903
pB 06 1000	686.0165	86.13359	31605.53	439995.7
PB 10 1000	359.0045	77.93355	31991.59	494690.9
pB 15 1000	1115.577	84.93359	54648.76	456623.3

pB 22 1000	1466.675	79.26689	72832.83	451037.3
pB 29 1000	1544.35	72.26685	78102.92	337811.5
pB 41 1000	2092.487	73.06685	106539.8	338218
pB 45 1000	2297.385	71.13351	118404.6	339307.4
pB 51 1000	2574.299	73.93353	131986.6	435405.1
pB 57 1000	2894.16	78.13355	146546.2	434678.5
pB 63 1000	2891.693	73.13352	148880.6	433347.9
pB 69 1000	3970.085	81.0669	202048.5	504548.6
PC 01 1000	740.1525	79.13355	189882.5	490261.1
PC 03 1000	321.0703	75.86687	42472.52	500224.8
pC 06 1000	215.335	81.60023	15257.01	444346.4
PC 10 1000	638.0143	83.33358	30012.03	497889
pC 15 1000	624.6803	84.00025	46355.92	453809
pC 22 1000	1258.855	81.33357	83897.68	468338
pC 29 1000	1571.753	71.80018	100839.1	337050.9
pC 41 1000	2445.143	73.86686	147942.8	334476.1
pC 45 1000	2762.334	72.06685	166619.7	331057.4
pC 51 1000	3225.764	73.06685	191983.3	439250.9
pC 57 1000	3633.862	77.33354	209891.8	432228
pC 63 1000	3953.414	79.13355	231842.2	430939.2
pC 69 1000	5084.638	80.6669	292735.3	497031
PD 01 1000	184.5345	74.93353	6224.089	493302
PD 03 1000	291.403	77.20021	11844.11	496112.2
pD 06 1000	487.5417	80.20023	21508.25	463981.2
PD 10 1000	898.4949	76.93354	43620.6	492966.5
pD 15 1000	845.025	82.33357	40667.08	447489.8
pD 29 1000	1176.782	71.26684	58443.39	333672.1
pD 41 1000	1669.764	70.73351	84610.72	329574.8
pD 45 1000	1914.395	69.80017	98547	335596.9
pD 51 1000	2399.202	67.40016	121463.5	437491.7
pD 57 1000	2845.95	76.60021	146402.6	427299.8
pD 63 1000	3556.509	76.53354	181944.2	440447.8
pD 69 1000	4380.472	80.06689	224470.5	484135.9

* The unit of the data in the table above is not listed. However, the unit is in fact not needed because when doing the calculation, it is always the ratio between two numbers that is used, thus avoiding the use of any unit.

Table 9 – Raw results of ICP-MS (deviation)

sample id	U-235	U-236	U-238	Th-232
GdB 01 100	13.38093	5.025512	169.232	4627.078
GdB 03 100	13.79567	3.500808	289.3593	3562.141

GdB 06 100	11.02987	4.303765	217.7197	5169.568
GdB 10 100	20.63838	3.543397	108.4988	4658.257
GdB 15 100	22.4117	7.421477	628.8862	8257.443
GdB 22 100	16.18472	3.832627	498.8785	3279.296
GdB 29 100	19.74896	7.220375	481.9877	4438.673
GdB 41 100	40.5605	4.167352	392.5491	4128.571
GdB 45 100	6.681123	4.44099	247.9114	2377.033
GdB 51 100	13.48026	2.975841	421.4012	4845.436
GdB 57 100	25.06075	2.126561	240.9088	1707.442
GdB 63 100	15.43811	1.386449	362.2202	2492.781
GdB 69 100	19.13104	4.125819	552.7503	5159.702
GdC 01 100	8.488843	3.939842	210.3845	4209.19
GdC 03 100	23.78593	3.911539	476.7224	4629.333
GdC 06 100	20.11119	7.262571	251.7762	4628.927
GdC 10 100	11.92747	4.222972	247.7916	5758.649
GdC 15 100	17.01117	2.911675	351.0968	7585.875
GdC 22 100	22.25769	4.037345	649.5726	7504.574
GdC 29 100	12.89683	4.960981	291.9777	2930.266
GdC 41 100	4.76467	5.383124	267.3604	3627.871
GdC 45 100	14.4715	5.51465	612.0539	5111.951
GdC 51 100	5.790037	1.725631	348.69	4151.298
GdC 57 100	14.8292	2.081675	410.8264	5096.25
GdC 63 100	4.180809	5.903885	496.8177	4312.582
GdC 69 100	21.51239	4.310214	1211.087	9534.935
GdD 01 100	8.694352	3.671228	261.4353	7958.532
GdD 03 100	13.45886	1.84693	351.6488	11832.99
GdD 06 100	11.27214	3.939847	233.8759	5682.88
GdD 10 100	5.434597	3.678788	631.0754	7167.464
GdD 15 100	8.808736	6.076399	1173.229	8374.308
GdD 22 100	3.749199	2.911679	535.7543	9670.812
GdD 29 100	14.96225	6.247692	619.861	6075.706
GdD 41 100	7.830431	2.701864	325.4017	4303.342
GdD 45 100	14.09271	4.444743	438.7631	3817.654
GdD 51 100	16.06068	1.885626	565.852	7276.093
GdD 57 100	11.32803	3.640835	661.7536	5940.401
GdD 63 100	25.17818	4.22034	1205.355	6550.294
GdD 69 100	32.92995	4.537519	1342.605	1667.537
GdE 01 100	51.60999	4.25574	911.4257	11121.9
GdE 03 100	42.0525	6.977782	1338.717	16265.03
GdE 06 100	21.17335	5.118622	588.0412	5773.892
GdE 10 100	19.69155	4.54975	197.8291	6876.909
GdE 15 100	29.91027	6.808532	527.1893	10621.24

GdE 22 100	22.64851	5.535775	539.9191	8154.278
GdE 29 100	16.80573	5.019983	235.6332	1783.059
GdE 41 100	22.85124	5.5608	252.7275	4500.021
GdE 45 100	19.02708	4.94977	393.4383	4480.148
GdE 51 100	3.277887	3.236954	27.4779	4578.691
GdE 57 100	10.28373	5.17797	517.3945	4149.026
GdE 63 100	34.86756	2.180734	593.4754	6874.586
GdE 69 100	22.08646	2.772897	995.9516	9427.611
GdF 01 100	1.855946	4.199229	163.8588	8113.999
GdF 03 100	15.06051	4.3372	207.0247	6393.888
GdF 06 100	7.455915	3.078617	241.7569	7112.018
GdF 10 100	5.423287	4.576534	170.2187	8303.806
GdF 15 100	8.25107	7.819534	242.8364	4566.559
GdF 22 100	7.481975	2.693629	375.6675	6834.419
GdF 29 100	5.10237	2.892532	203.212	4621.054
GdF 41 100	5.167301	5.024406	167.8903	4512.149
GdF 45 100	9.738433	5.609542	205.3812	1430.316
GdF 51 100	1.633001	3.819557	8.500602	3600.788
GdF 57 100	8.623171	7.045125	296.833	6702.969
GdF 63 100	17.76842	6.229885	325.6004	3486.711
GdF 69 100	8.016184	4.207155	317.1803	7790.659
pA 01 1000	43.72428	5.192984	7287.824	2726.042
pA 03 1000	54.8776	6.396223	4644.78	4459.694
pA 06 1000	16.216	5.934859	749.6244	5756.076
pA 10 1000	32.55863	6.527753	4582.842	5187.176
pA 15 1000	36.36877	4.147319	7275.082	7329.258
pA 22 1000	14.81789	6.375347	2758.034	2898.769
pA 29 1000	26.88035	7.55577	5702.354	3412.683
pA 41 1000	29.91204	4.929533	4862.696	2569.563
pA 45 1000	35.4837	5.30726	3853.92	5158.771
pA 51 1000	39.26228	5.150005	3051.204	5250.914
PB 01 1000	11.38347	3.749094	186.6683	6874.581
PB 03 1000	10.19939	4.729367	305.4892	5518.041
pB 06 1000	16.84652	7.143806	423.926	9016.264
PB 10 1000	10.79122	2.975845	500.328	11108.9
pB 15 1000	32.54877	2.985166	1019.057	9573.556
pB 22 1000	36.43812	8.115189	2006.629	10732.16
pB 29 1000	22.27769	1.673328	393.2563	4417.069
pB 41 1000	36.00142	4.36147	925.6889	3312.889
pB 45 1000	59.58046	5.05857	2599.194	6936.607
pB 51 1000	37.41175	5.504572	675.9492	6667.122
pB 57 1000	65.77495	5.485364	1896.593	7245.943

pB 63 1000	64.09152	3.185051	1856	8153.875
pB 69 1000	47.80773	9.004371	1729.373	2901.799
PC 01 1000	6.922945	5.918928	2922.953	4753.086
PC 03 1000	11.4419	2.501124	437.3138	8036.309
pC 06 1000	8.653967	1.920659	208.0387	10014.44
PC 10 1000	23.82565	4.314084	426.2452	6414.372
pC 15 1000	8.775349	4.209802	1128.505	6059.636
pC 22 1000	26.95771	4.390672	1241.033	7157.967
pC 29 1000	21.11841	5.102313	627.9341	5606.897
pC 41 1000	60.18285	4.413387	1597.738	3873.293
pC 45 1000	47.84133	4.680954	1790.15	4139.052
pC 51 1000	83.95651	2.660423	3575.714	10211.9
pC 57 1000	65.20776	3.027667	3799.727	8402.976
pC 63 1000	95.75523	3.404264	3598.539	7483.818
pC 69 1000	69.34013	6.59549	4778.314	8732.493
PD 01 1000	7.890318	3.328347	45.59857	7394.304
PD 03 1000	9.029153	4.305059	246.6826	10396.79
pD 06 1000	22.96767	0.9006222	263.8483	4483.314
PD 10 1000	7.18686	8.470254	1147.665	7672.8
pD 15 1000	15.76481	6.912186	513.92	7185.046
pD 29 1000	38.52984	3.361564	777.2518	3495.112
pD 41 1000	44.73963	6.130103	1029.786	4420.186
pD 45 1000	38.65631	2.609824	1538.79	3916.447
pD 51 1000	65.41694	8.371288	1576.064	7087.854
pD 57 1000	50.53226	3.825374	2316.29	6427.952
pD 63 1000	40.05816	5.723278	2670.275	8084.541
pD 69 1000	73.40195	2.553879	4648.751	8926.503